Integrated Modeling of Steady-state Scenarios and Heating and Current Drive Mixes for ITER

M. Murakami[1], J.M. Park[1], G. Giruzzi[2], J. Garcia[2], P. Bonoli[3], R.V. Budny[4], E.J. Doyle[5], A. Fukuyama[6], N. Hayashi[7], M. Honda[7], A. Hubbard[3], S. Ide[7], F. Imbeaux[2], E.F. Jaeger[1], T. Luce[8], Y-S. Na[9], T. Oikawa[10], T.H. Osborne[8], V. Parail[11], A. Polevoi[10], R. Prater[8], A.C.C. Sips[12], J. Snipes[10], H.E. St. John[8], P.B. Snyder[8], I. Voitsekhovitch[11], and ITPA/Integrated Operation Scenario Group

[1]Oak Ridge National Laboratory, P.O. Box 2008, Oak Ridge, Tennessee 37831, USA
[2]CEA, IRFM, F-13108, Saint-Paul-lez-Durance, France
[3]Plasma Science and Fusion Center, MIT, Cambridge, Massachusetts 02139, USA
[4]Princeton Plasma Physics Laboratory, P.O. Box 451, Princeton, New Jersey 08543, USA
[5]University of California, Los Angeles, California 90095, USA
[6]Graduate School of Engineering, Kyoto University, Kyoto, Japan
[7]Japan Atomic Energy Agency, Naka, Ibaraki-ken, 311-0193 Japan
[8]General Atomics, San Diego, California 92186-5608, USA
[9]Dept. Nuclear Engineering, Seoul National University, Seoul, 151-744, Korea
[10]ITER Organization, Route de Vinon sur Verdon, 13115 Saint Paul lez Durance, France
[11]EURATOM/CCFE Fusion Association, Culham Sci. Centre, Abingdon, OX14 3DB, UK
[12]EFDA-CSU, Culham Science Center, Abingdon, OX14 3DB, UK

e-mail contact of main author: murakamim@ornl.gov

Abstract. Recent progress on ITER steady-state scenario modeling by the ITPA-IOS group is reviewed. Code-to-code benchmarks as the IOS group's common activities for the two steady state scenarios (weak shear scenario and internal transport barrier scenario) are reviewed. These are discussed in terms of transport and kinetic profiles, heating and CD sources using various transport codes. Here weak magnetic shear scenarios integrate the plasma (core to edge) by combining a theory-base (GLF23) transport model with scaled experimental boundary profiles. The edge profiles (ρ=0.8–1.0) are adopted from edge localized mode-averaged analysis of a DIII-D ITER Demonstration discharge. Uncertainties are estimated based on theoretical instability limits and experimental scaling laws, underscoring uncertainties in predicting pedestal and transport for ITER. A fully noninductive steady-state scenario is achieved with fusion gain Q=3.4, noninductive fraction f_{NI} = 1.01, bootstrap current fraction f_{BS} = 0.64 and normalized beta β_N = 2.8 at plasma current I_p = 8 MA and toroidal field B_T = 5.3 T using ITER day-1 heating and current drive (CD) capability. Operation at 9 MA to achieve Q=5 would lack 1–2 MA of noninductive current using the day-1 current drive systems. However, based on the calculated, fully-relaxed loop voltage, the long pulse operation goal (3000 s) with Q=5 at I_p = 9 MA is possible if a sufficient flux (15–30 Weber) remains in the poloidal field system for the steady-state burn phase. A number of steady state scenarios with different heating and current drive mixes in a wide range of conditions were explored by exploiting the steady-state solution procedure for the GLF23 transport model. Source calculations in these simulations have been revised for electron cyclotron current drive including momentum conservation effects and for neutral beam current drive with finite orbit and magnetic pitch effects.

1. Introduction

One of the primary goals of the ITER project is to demonstrate reactor scale steady-state (SS) operation for future tokamak reactors [1], specifically to achieve simultaneous operation with fully noninductive current drive (noninductive current fraction f_{NI} = 100%) with fusion gain $Q \geq 5$ and high bootstrap current fraction for pulse length ~3000 s. This is very challenging because the operational space for ITER is restricted by many other physical and engineering limits, such as beta limit, power loss to the diverter, heat and particle handling, and heating and current drive (H&CD) limitations. Optimization of the ITER performance requires integrated modeling tools to allow for these complex interactions.

We report here progress on ITER steady-state scenario modeling efforts by the International Tokamak Physics Activity (ITPA) – Integrated Operation Scenario (IOS) Topical Group. Benchmarking of various transport code simulations are carried out as

common activities of the IOS group for two types of steady state scenarios: weak magnetic shear scenarios (type-A), and scenarios with strongly reversed magnetic shear (type-B). Weak reverse shear steady state scenario developed with a scaled experimental edge is described together with their limitations and uncertainties in ITER predictions. We then examine the impact of different H&CD mixes for achieving the steady state objective.

2. Code-to-Code Benchmark

2.1 Benchmark for Weak Magnetic Shear Scenario

Good progress has been made in the code benchmark based on a scenario that integrates the core and edge by combining the theory-based (GLF23) model with scaled experimental boundary conditions. The objectives of benchmarks are to benchmark the specific GLF23 transport model [2], fusion power calculations, H&CD [neutral beam (NB), electron current (EC), fast wave (FW)] modules, and equilibria among different code implementations. In addition, we intend to study effects critical to steady-state scenario development, such as: (i) current profile evolution at f_{NI}~1, (ii) the role of on-axis current drive [fast wave current drive (FWCD)] and q_0 behavior; and (iii) the relaxation time to a stationary state. Simulations of the steady-state operation mode are done using fixed-boundary 1.5D transport codes including FASTRAN/ONETWO [3,4]; TRANSP [5]; CRONOS [6]; TOPICS-IB [7], and ASTRA [8–10].

Other significant assumptions are fixed for the different code simulations as the benchmark "guideline". Since the GLF23 model is strongly affected by the boundary conditions, the most important assumption is the boundary (including the pedestal) specification. An edge localized mode (ELM)-averaged edge profile scaled from that of an ITER SS demonstration DIII-D discharge [11] was adopted near the boundary (ρ= 0.8–1.0), as described in Sec. 3. The guidelines, together with all relevant profiles and equilibria, were distributed to various group members and interested others. The operating current and field are I_p = 8 MA and B_T = 5.3 T. As in the previous benchmark studies for the hybrid scenario [12], the DT fuel ion ratio is assumed to be 50–50. The impurities are Be and Ar, with assumed fractions of 2% and 0.12%, respectively. The impurity density profile shapes are forced to be the same as the electron density, while the impurity temperatures are set equal to the main ion temperatures. The electron density profile is prescribed to be flat in the core ($\rho \le 0.8$), giving Greenwald number N_{GW}=0.85 with the boundary profiles ($0.8 \le \rho \le 1.0$) specified. The fuel ion density profiles are determined from quasi-neutrality. The ratio of the effective particle to energy confinement time (τ_p^* / τ_E) is enforced to be 5. The injected powers are the day-1 H&CD: N-neutral beam injection (NBI) (1 MeV, 33 MW, steered to full off-axis), ion cyclotron resonance frequency (ICRF) heating (20 MW, 53 MHz, 90-deg phasing) and EC heating and current drive (170 GHz, 20 MW, equatorial launch steered for off-axis CD (poloidal steering angle α=0, and toroidal steering angle β=35°). The GLF23 model [2] is used with *ExB* shear multiplier of 1.0. Momentum diffusivity is given by the GLF23 model with twice Chang-Hinton neoclassical ion thermal diffusivity [13].

Figure 1 shows comparison of the transport and kinetic profiles obtained from simulation codes and Table I shows the comparison of the global parameters. Excellent agreement has been achieved for the predicted T_e and T_i profiles using the GLF23 transport model among the different codes. The profiles reached in long pulse by various time-dependent simulations agrees with the steady state solution obtained by FASTRAN/ONETWO. The resulting T_e and T_i profiles are totally insensitive to *ExB* stabilization, so that only the magnetic shear (rather than rotational shear) impacts confinement (with H_{98y2} = 1.5). Although the global MHD stability is yet to be assessed, even a modest rotation, however, could benefit resistive wall mode (RWM) stability.

TABLE I. Scalar parameters for benchmarking of the weak shear steady-state scenario.

Code	T_{e0} (keV)	T_{i0} (keV)	I_{BS} (MA)	I_{NB} (MA)	I_{EC} (MA)	$1/2I_{FW}$ (MA)	f_{NI}	Q	Pα (MW)	Wα (MJ)	β_N	H_{98}	H_{89}	q_{min}
FASTRAN	22.94	20.12	5.0	2.33	0.80	0.35	1.06	3.31	48.03	17.10	2.75	1.49	3.04	1.72
TRANSP	23.49	19.91	4.39	2.29	0.87	0.33	0.99	3.31	48.86	17.24	2.60			1.90
TOPICS	22.27	18.73	4.23	2.94	0.68	0.35	1.03	3.26	47.62	16.64	2.63	1.48		1.81
CRONOS	20.0	19.7	4.60	3.00	0.60	0.31	1.10	3.80	55.00		2.30	1.30	2.30	2.1
ASTRA.p	22.7	2.0	4.12	3.26	0.60	0.37	1.04	3.34	49.2	19.0	2.70	1.36	3.16	1.85
ASTRA.n	21.88	18.93	4.14	3.05	0.79	0.37	1.04	3.03	44.12		2.37	1.52		1.80

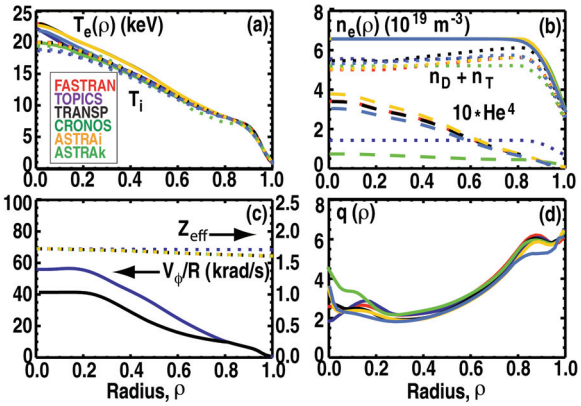

FIG. 1. Results of code-to-code benchmarking for the ITER weak-shear steady-state scenario. Profiles calculated by different codes are compared for: (a) electron and ion temperature, (b) electron, ion, and helium-4 density, (c) effective charge and toroidal angular velocity, (d) safety factor. FASTRAN/ONETWO denoted as FASTRAN; ASTRA implemented in ITER as ASTRAi [9]; and ASTRA implemented in KSTAR as ASTRAk [10].

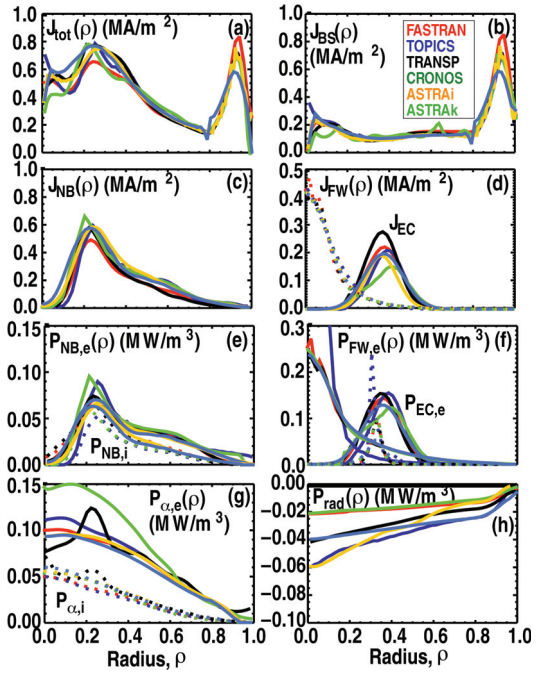

FIG. 2. Results of code-to-code benchmarking for the ITER weak-shear steady-state scenario. Profiles calculated by different codes are compared for: (a) total current, (b) bootstrap, (c) NBCD, (d) FW and ECCD current density, (e) NB power to electrons and ions, (f) electron cyclotron power to electrons and fast wave power to electrons and ions, (g) alpha power to electron and ions, and (h) total radiation power loss (with negative sign representing the power loss).

Figure 2 shows comparison of heating and current drive profiles from the various sources. There are some differences in edge bootstrap current possibly due to differences in density profile, resulting in difference in edge q-profile. Monte-Carlo orbit following codes are needed to calculate off-axis neutral beam current drive (NBCD) correctly, taking into account the alignment of the NB injection with the magnetic pitch [14,15]. We need to check the directions of I_p and B_T and NBI direction that are known to cause difference of about 10% in CD values. Although good agreement is found between NUBEAM [16] (in FASTRAN/ONETWO and TRANSP) and TOPIC-IB, the machine direction and sign of B_T and I_P should be rechecked. Accurate electron cyclotron current drive (ECCD) calculations should conserve parallel momentum between electron collisions [17,18]. Full momentum conservation code (CQL3D [9]) calculates ECCD by factors of 1.1–1.4 larger than that calculated by codes without momentum conservation (TORAY-GA [20]) under the ITER conditions. The difference in ECCD (FASTRAN/ONETWO and TRANSP versus TOPICS and CRONOS) is due to the momentum conservation effects.

FWCD was calculated using the ray-tracing CURRAY code [21] and full-wave codes (CRONOS [6] and ASTRA [9]). The CURRAY results were benchmarked with the full-wave

AORSA3D code [22]. The comparison of integrated power fractions shown in Table II suggest that the reduced CURRAY model may be satisfactory in these calculations. There are large variations of radiation profiles that need to be resolved.

TABLE II. Benchmark between full-wave AORSA and ray tracing CURRAY codes. CURRAY-1 includes beam and alpha absorption, while CURRAY-2 does not.

	AORSA	CURRAY-1	CURRAY-2
P (electron) (%)	64.26	72.70	82.40
P (D-thermal) (%)	0.40	1.35	0.15
P (T-thermal) (%)	32.83	19.50	21.10
P (D-beam) (%)	0.98	7.45	0.25
P (Alpha) (%)	1.48	0.19	0.00
P (He^{4}) (%)	0.04	0.00	0.00
P (Impurity (%)	0.02	0.00	0.00
I(FWCD) (kA)	603.00	645.00	654.00

2.2 Benchmark for Internal Transport Barrier Scenario

The second steady-state scenario is the scenario with an ion transport barrier (ITB) in the core. In ITER, ITBs would be associated with negative magnetic shear due to the lack of a rotational shear. Here control of current density profile is essential, but this is quite complicated when the bootstrap current becomes dominant. A conceptual solution is to use ECCD to lock the bootstrap current profile. CRONOS simulations [23,24] use a prescribed heat diffusivity similar to that used in the official scenario-4 [1] in which a shear function reduces transport whenever the shear is negative. In order to sustain the ITB, any large amount of CD inside the ITB is observed to cause deleterious effects, prohibiting the use of NBI within the ITB. A scenario at 8 MA, f_{BS}=75%, f_{NI}=95%, and Q=6.5 were developed using rf current drive alone (20 MW of ICRF, 20 MW of ECCD, and 12 MW of LHCD). ITB was sustained for 2000 s, and was characterized by critical transition phenomena and the existence of threshold value for ECCD [23]. The profiles are shown in Fig. 3.

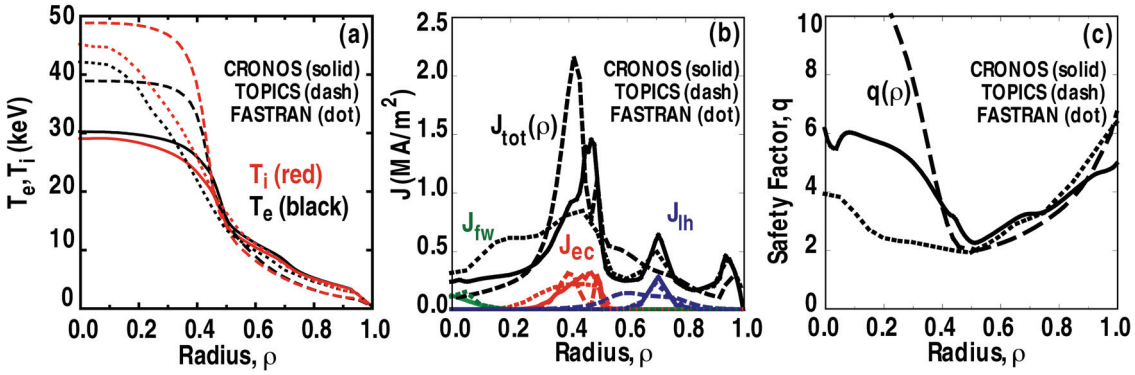

FIG. 3. Results of benchmarking for ITER steady-state ITB scenarios. Profiles calculated by three codes are compared for profiles of: (a) electron and ion temperature; (b) total current density and external CD sources: fast wave, electron cyclotron and lower hybrid CD; and (c) safety factor.

It was proposed to reproduce the CRONOS scenario using other codes. TOPICS-1B simulation [7] with the same ECCD launcher to that used in CRONOS shows ITB shrinkage without achieving stationary state due to split (double-humped) ECCD (owing to Shafranov shift resulting from large α-heating). Additional outward aiming of EC deposition from a top launcher together with LH was used to lock the outer ITB location. Although this made it steady state, the temperature ITB profiles are different from that obtained by CRONOS.

The ITB scenario was reproduced by the steady-state solution procedure [3] using ECCD. Robust stationary (fully relaxed) ITB was generated using the same ECCD as the guideline. But simulations show ITB is different from CRONOS in that the strength of the ITB depends on the width and height of the ECCD profile. With a broader ECCD deposition, weak ITB

was generated in steady state. This is interesting because ECCD broadness may provide control over the MHD stability and confinement. It is interesting to note that in high-β, steady-state experiments in DIII-D, broad (rather than narrow) ECCD deposition leads to a more stable discharge without n=1 mode [25], The stability improvement is not believed to be due to ECCD control of neoclassical tearing mode (NTM), but more likely due to better control of Δ'. Further studies will be carried out on the issue of sustainability of an ITB by broadening the ECCD.

3. Optimization of Weak Magnetic Shear Scenarios

Recent advances in the weak magnetic shear using the theory-based (GLF23) have been: (i) treatment of the boundary conditions (scaled from experiment rather than required to achieve the goal) which affects some conclusions; (ii) a new efficient steady state solution procedure whose results are benchmarked successfully with a number of time-dependent transport codes as discussed earlier and can find an application in heating CD mix studies; and (iii) updated H&CD calculations, in particular ECCD and NBCD.

Weak magnetic shear scenario is developed using theory-based GLF23 model [2] with a scaled experimental boundary condition. The edge (normalized radius, ρ=0.8–1.0) profiles for this scenario are adopted from ELM-averaged analysis of a DIII-D ITER Demonstration discharge [11]. The edge scaling is based on the thermal normalized beta profile $\beta_N^{th}(\rho)$ that has been shown to be self-similar across tokamaks. An iterative steady state (d/dt=0) solution procedure has been developed using a new fast transport solver FASTRAN [3] with the ONETWO [4] and EFIT [26] codes.

A fully noninductive steady state scenario (type-A baseline) is achieved at plasma current I_p = 8 MA and toroidal field B_T = 5.3 T, as shown in Fig. 4. The noninductive current fraction f_{NI} = 101% with fusion gain Q=3.4 and β_N = 2.8 with bootstrap current fraction f_{BS} = 64% was achieved using the ITER day-1 H&CD capability. There is no current evolution with nearly zero loop voltage V_{loop} (-0.4 mV), demonstrating fully steady state. Only half of the full FWCD capacity was used in the simulation to avoid the over-drive of noninductive current near the axis. High normalized H-mode confinement H_{98y2} = 1.5 is obtained without *ExB* shear stabilization. The steady state solution based on the above procedure was benchmarked successfully with profiles from time-dependent transport codes, as described earlier.

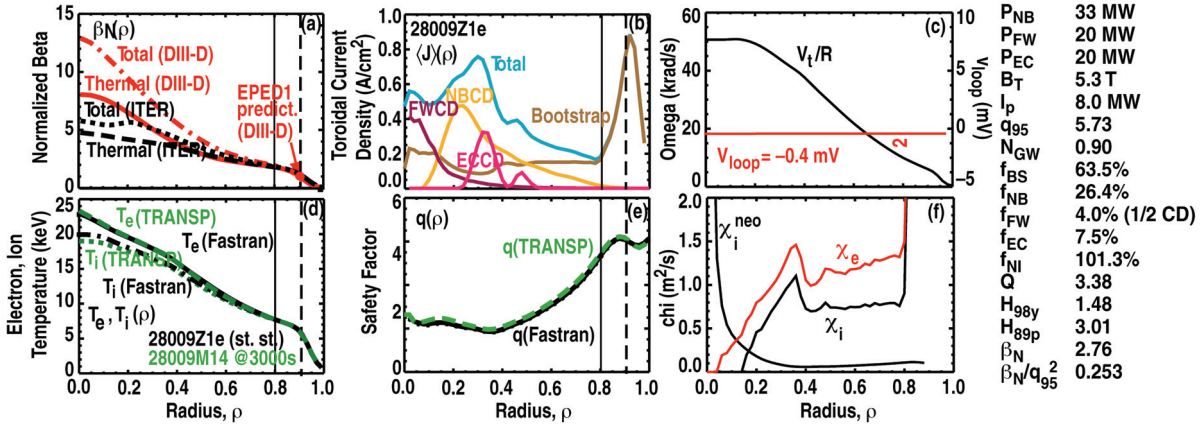

FIG. 4. ITER weak-shear steady-state profiles from the GLF23 model with the experimental boundary conditions at ρ=0.8–1.0 from a DIII-D ITER Demo discharge (red). The theoretical pedestal model (EPED) predicts β_{Nped} = 0.91 at ρ_{ped} = 0.905 (dashed line), while the experimental β_{Nped} is ≈10% higher at the same ρ_{ped}. The profile of the SS solution procedure agrees well with the profile time-dependent TRANSP (t = 3000 s) (green).

The main uncertainties are whether the high performance operating point from the present database of pedestal and transport can be extrapolated to those in different parameter regimes (e.g., reduced plasma rotation, $T_e/T_i \approx 1$, density peaking). Extrapolations from the present experiment to ITER serve to put bounds on the uncertainties. The theoretical prediction, the EPED model [27], for pedestal width and height combines the peeling-ballooning mode stability constraint and the kinetic ballooning mode width scaling (proportional to square-root of poloidal beta) to determine the pedestal height. For the ITER case, the theoretical prediction is that the peeling-ballooning threshold is ~25% below the simulation β_N^{ped} (=1.20) at the top of the pedestal ($\rho^{ped} = 0.91$). However, the recent pedestal normalized gyro-radius (ρ^*) similarity experiments on DIII-D/JET indicates some favorable prospect for ITER. Preliminary experimental analysis of the H-mode edge transport barrier (ETB) in the JET and DIII-D found a weak inverse ρ^* (normalized ion gyro-radius) dependence of pedestal width, ruling out positive ρ^* dependence that most theory-based models predict [28]. Although the experimental analysis is still underway, the uncertainties of pedestal width and height normalized to EPED predicted values range at about ±20%. The β_N^{ped} used for simulation corresponds to an upper end of the experimental uncertainty range. This tends to compensate the GLF23 model predictions that are known to be pessimistic among the available transport models.

4. Impacts of H&CD Mixes and Upgrade on ITER Steady-State Scenarios

Operation space for f_{NI} and Q with different H&CD mixes has been studied in a wide range of conditions by exploiting the steady-state solution procedure discussed earlier. Figure 5 shows the operational space (f_{NI} vs Q) with different H&CD mixes, including ITER H&CD upgrade options. About 30 ITER steady-state scenarios have been evaluated with different H&CD mixes. The following observations are made, as described in detail elsewhere [21].

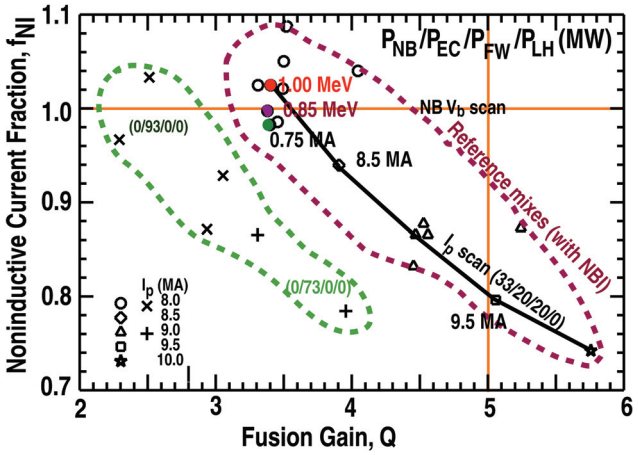

FIG. 5. Noninductive fraction (f_{NI}) vs fusion gain (Q) for various scenarios with different I_p and H&CD mixes in the weak shear regime. Higher Q values are obtained with high I_p and NBCD-mixed scenarios, but f_{NI} is 0.85-0.9 without NB upgrade.

- The plasma current scan with the day-1 H&CD shows the trade-off between f_{NI} and Q. The higher I_p operation (I_p = 9 MA) would be important to reach the Q=5 objective, but the remaining ohmic current of 1–2 MA may have to be replaced with a new source.
- Based on the calculated, fully-relaxed loop voltages, if sufficient (15–30) volt-seconds remain in the poloidal field system, long-pulse, steady burn operation for much longer than 3000 s is possible with Q~5 at I_p = 9 MA. The discharges with finite ohmic current will reach the pulse length goal and will play an important role in developing steady-state scenarios and preparing for the engineering test phase of ITER.
- Electron cyclotron heating (ECH) [or ECH plus ion cyclotron heating (ICH) gives at best f_{NI}~80% and Q~4. Ninety-three megawatt power of ECCD would be needed to get full noninductive but then at Q~2.

- For NBI, the driven current is not that sensitive to beam voltage at fixed power, as one could still use 850 kV injection at a penalty of ~5% NBCD. An increase in ECCD power (by <10 MW) can compensate the reduction of f_{NI}.
- Direct ion heating with ICRF is advantageous in increasing Q and f_{NI}. Ion heating using He^3-minority ICRF (about 55% to He^3 and 5% to 2nd harmonic T) contributes to increasing Q_{DT}.

In the ITER Engineering Test Phase, high neutron fluence is needed to test engineering components. High DT neutron power and long pulse operation are needed, and the H&CD upgrade is mainly for that purpose. Since the noninductive fraction itself is a good proxy for the pulse duration, we plot f_{NI} vs DT neutron power for various upgrade options in Fig. 6.

- Scenarios with NBI achieve the highest f_{NI} again, but also observe that a combination with higher power ECCD (40 MW) enables high DT power with full noninductive operation. NBCD is good to provide the majority of the current needed off-axis, while off-axis ECCD is good for tailoring the current profile for better stability or confinement.
- LHCD can increase f_{NI} at radii larger than the present N-NBI system can reach, but its heating and thus CD are penalized by being far off-axis. Preliminary scenarios with LHCD were calculated using fixed LHCD profiles calculated by CRONOS [6] and GENRAY/CQL3D [30] and ACCOME [31,32] with parallel refractive index $n_{\|} = 2.0$ to 1.8.

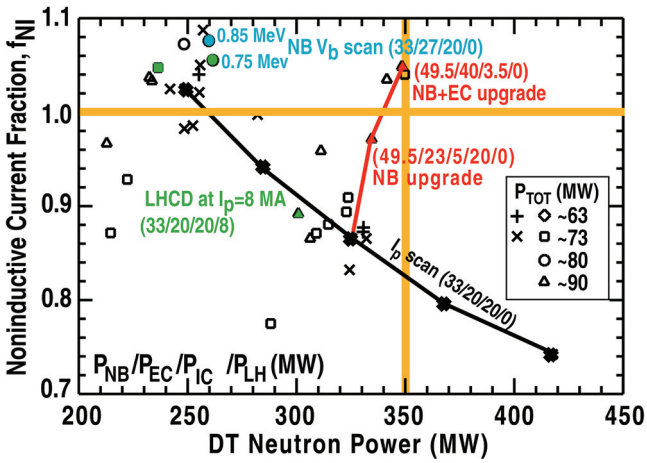

FIG. 6. Noninductive fraction vs DT neutron power predicted by the GLF23 model simulation for the weak shear regime using possible ITER heating and CD upgrade options as well as baseline H&CD mixes. Combination of NB and ECCD could achieve the target DT neutron power of 350 MW for ITER engineering studies with full NI operation at I_p = 9 MA.

5. Conclusion

Recent progress on ITER steady-state scenario modeling by the ITPA-IOS group is reviewed. Progress in code-to-code benchmarking for two steady-state scenarios (weak shear scenario and internal transport barrier scenario) was discussed in terms of transport and kinetic profiles, and heating and CD sources using the transport codes as the IOS group's common activity. A new weak magnetic shear scenario was developed using a theory-based GLF23 model with scaled experimental boundary conditions. A fully noninductive steady state scenario was achieved at 8 MA with Q=3.4. Operation to achieve Q=5 would lack 1–2 MA of noninductive current using the day-1 CD system. The operation spaces for f_{ni} and Q and DT neutron power with different H&CD mixes was examined over in a wide range of conditions. Source calculations in these simulations were improved for ECCD and NBCD.

This work was supported by the US Department of Energy under DE-AC05-00OR22725, DE-AC02-09CH11466, DE-FG02-08ER54984, and DE-FC02-04ER54698. We wish to acknowledge useful discussions with Drs. C.E. Kessel, T.S. Taylor and M.R. Wade. Some of the authors benefited from discussions with the AG-2 Working Group members, in particular, Drs. F. Wagner, O. Sauter, and H. Zohm. The modeling was carried out in part using Grid-enabled TRANSP on the National Fusion Grid, and we would like to thank the members of the National Fusion Collaboratory Project at PPPL and GA (www.fusiongrid.org) sponsored by the US DOE SciDAC Program. The views and opinions expressed herein do not necessarily reflect those of the ITER Organization (<https://user.iter.org/?uid=2LL67W).

References

[1] GORMEZANO, C., et al., Nucl. Fusion **47** (2007) S285
[2] WALTZ, R.E., et al., Phys. Plasmas **4** (1997) 2482; and hppc://w3.pppl.gov/NTCC/GLF.
[3] PARK, J.M., et al., 3rd ITPA IOS TG Mtg (Frascati, 2009); "Extrapolation of ITER Demo Discharges Using Theory-Based Models," to be submitted to Nucl. Fusion; PARK, J.M., this conference, EXC/P2-05
[4] ST JOHN, H.E., et al., Plasma Phys. Control. Nucl. Fusion Research 1994 (Proc. 15th Int. Conf., Seville, 1994) Vol. 3 (IAEA, Vienna, 1995) p. 603
[5] HAWRYLUK, R.J., "An Empirical Approach to Tokamak Transport," in *Physics Close to Thermonuclear Conditions*, edited by B. Coppi et al. (Commission of the European Communities, Brussels, 1980) Vol. 1, p. 19
[6] ARTAUD, J.F., et al., Nucl. Fusion **50** (2010) 043001
[7] SHIRAI, H., et al., Plasma Phys. Control. Fusion **42** (2000) 1193; HAYASHI, N., et al., Nucl. Fusion **45** (2005) 933; and HAYASHI, N., this conference
[8] PEREVERZEV, G., et al., IPP-Report IPP 5/98 (2002)
[9] POLEVOI, A., et al., JAERI-Data/Code 97-014 (1997)
[10] NA, Y-S, et al., Nucl. Fusion **49** (2009) 115018
[11] DOYLE, E.J., et al., Nucl. Fusion **50** (2010) 75005
[12] KESSEL, C.F., et al., Nucl. Fusion **47** (2007) 1274
[13] CHANG, C.S., and HINTON, F.L., Phys. Fluids **25** (1982) 1493
[14] MURAKAMI, M., et al., Fusion Sci. Tech. **54** (2008) 994
[15] PARK, J.M., et al., Phys. Plasmas **16** (2009) 092508
[16] PANKIN, A., et al., Comput. Phys. Commun. **43** (1981) 61
[17] PRATER, R., et al., Nucl. Fusion **48** (2008) 035006
[18] MARUSHCHENKO, N., et al., "Progress in ECCD Modeling: Parallel Momentum Conservation and Finite Collisionality Effects," accepted for publication in Phys. Plasmas (2010)
[19] HARVEY, R.W. and McCOY, M.G., in Proc. IAEA Tech. Com. Mtg 1992 (IAEA, Vienna, 1993) p. 498
[20] LIN-LIU, Y.R., et al., Phys. Plasmas **10** (2003) 4064
[21] MAU, T.K., et al., *Radio Frequency Power in Plasmas: 13th Top. Conf.*, American Institute of Physics, Conf. Proc. **485**, New York, 1999, p. 148
[22] JAEGER, E.F., et al., *Radio Frequency Power in Plasmas: 14th Top. Conf.,* American Institute of Physics, Proc. **595**, New York, 2001, p. 369
[23] GARCIA, J., et al., Phys. Rev. Lett. **100** (2008) 255004
[24] GIRUZZI, G., et al., 21st IAEA Fusion Energy Conf. (Geneva, 2008) paper IT/P6-4
[25] LUCE, T.C., et al., this conference, ITR/1-5
[26] LAO, L.L., et al., Nucl. Fusion **30** (1990) 1035
[27] SNYDER, P.B., et al., Phys. Plasmas **16** (2009) 056118; and SNYDER, P.B., this conference, THS/1-1
[28] OSBORNE, T.H., et al., H-mode Workshop (2010); and OSBORNE, T.H., this conference, EXC/2-1
[29] WAGNER, F., et al., "On the Heating Mixes in ITER," to be published in Plasma Phys. Control. Fusion (2010); WAGNER, F., this conference
[30] WILSON, J.R., et al., Nucl. Fusion **49** (2009) 115015
[31] TANI, K and DEVOTO, R.S., J. Comp. Phys. **98** (1992) 332
[32] BONOLI, P., et al., Plasma Phys. Control. Fusion **39** (1997) 223; this conference